Acta Technica 62 (2017), No. 6A, 529–538

Research on double closed loop control of large synchronous motor based on static inverter

Ming Chen[1], Yeting Liang[2]

Abstract. AC synchronous motor, because of its high power factor and high efficiency, is the leading player in the field of high-power electrical drive. Commutator motor is suitable for synchronous motor's soft start and speed regulation.The static frequency converter is the main starting equipment in the operation of the large synchronous motor.By producing the AC power supply whose frequency rise from zero to rated frequency with thyristor frequency converter, the static frequency converter synchronously starts the unit, integrates the unit into the power grid when the unit gradually reaches rated speed and meets the synchronous conditions, and at the same time disconnect frequency converter, hence the start operation is finished. Yet, start control policies are critical technical issues. This paper proposes double closed loop control to be used on static frequency converters.

Key words. rotor position detection, Synchronous motor, PID control, Load commutation.

1. Introduction

AC synchronous motors are widely used in large oil and gas transmission, marine propulsion, pumped storage and national wind tunnel tests and other high-power industrial occasions. In steelmaking industry in particular, large synchronous motors with high momentum of inertia are of critical importance and are widely used for such major production equipment as large blast furnace blowers, gas compressors for gas power generation and compressors for oxygen production and their power generally exceeds dozens of megawatt. Incomplete statics indicate that total installed capacity of synchronous motors in steelmaking industry exceeded 60000MW by the end of 2009 and is increasing by approx [1]. 5000MW every year. As scale of production of domestic steelmaking industry is constantly growing, the increment is also further increasing.

[1]School of Automotive and Traffic Engineering, Hubei University of Arts and Science, Xiangyang Hubei China 441053

[2]Wuhan R&D Center, Big Pawer Electrical Technology Xiangyang Co., Ltd., Wuhan Hubei China 430074

Among starting modes of large synchronous motors, static frequency converters (SFC) are featured with such incomparable advantages as soft starting, little power grid interference, smooth speed rise and highly automated and reliable program. By producing the AC power supply whose frequency rise from zero to rated frequency with thyristor frequency converter, the SFC synchronously starts the unit, integrates the unit into the power grid when the unit gradually reaches rated speed and meets the synchronous conditions, and at the same time disconnect frequency converter, hence the start operation is finished. Yet, start control policies are critical technical issues. This paper proposes double closed loop control to be used on SFCs.

2. Synchronous motor SFC control system

Figure 1 shows synchronous motor SFC control system diagram. The rotor position detection link realizes determination of range of the rotor position by detecting terminal voltage zero crossing. Speed loop output serves as setting of inner current loop and output of the current regulator after the signal of error between speed loop output and DC feedback value serves as thyristor trigger phase-shift signal. Control of constant inverter lead angle γ_0 ensures reliable conversion of the inverter and frequency and phase of synchronous motor stator current are determined by inverter output.

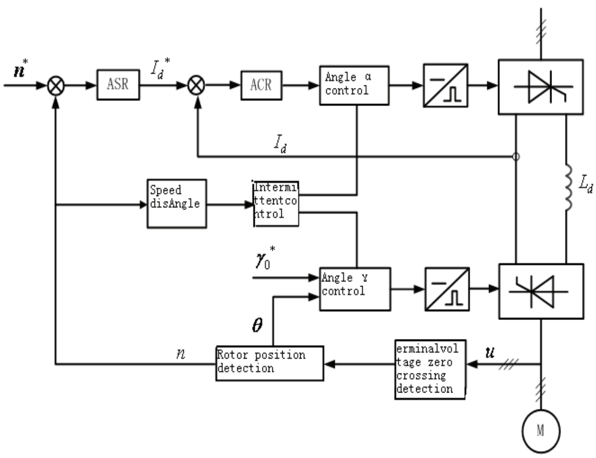

Fig. 1. Synchronous Motor SFC Control System Diagram

It can be seen that system control principle is similar to that of DC motor start control. With the speed and current double closed loop control, the system keeps the maximum operating current output through starting and acceleration processes. Besides, if thyristor based speed regulation system of synchronous motor is adopted, considering that DC side current directly affects converter output torque after the synchronous motor switches to high speed, this paper will focus on double closed loop control in the control system and scheme design.

3. Transfer function model of the static variable frequency speed regulation system

Figure 2 shows main loop of the static variable frequency speed regulation system. R_Σ is equivalent resistance of the main loop, consisting of filter reactor resistance, resistances of both phases of armature winding and equivalent resistance of thyristor forward voltage drop, etc.; U_D is the average value of the DC voltage u_D output by the bridge rectifier in steady state; E_D is the average of back EMF converted to inverter DC side DC potential e_D in steady state.

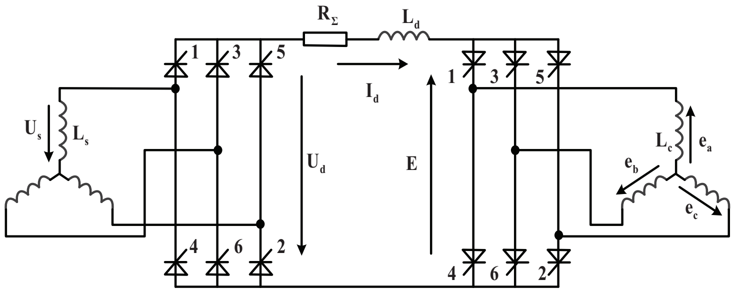

Fig. 2. SFC Main Loop Model

3.1. Bridge rectifier transfer function

$$G(s) = \frac{K_s}{T_s s + 1}\,, \tag{1}$$

Where T_s is lag time constant of the rectifying device, namely, average runaway time of the bridge rectifier, and for three-phase bridge circuit, $T_s = 0.00167$s; K_s is amplification factor of the three-phase bridge rectifier.

In view of commutation overlap angle, relationship between output DC voltage U_d of the three-phase bridge rectifier and AC side phase voltage rms u_s can be expressed as the formula below:

$$U_D = \frac{3\sqrt{6}}{\pi} U_s \cos(\alpha + \frac{\mu_s}{2}) \cos(\frac{\mu_s}{2})\,. \tag{2}$$

Since commutation overlap angle μ_s of the bridge rectifier is quite small under normal conditions, $U_D \approx 2.34 U_s \cos\alpha$, where U_s is AC side phase voltage rms. For digital control system, DC bus voltage may be obtained with the above formula and $K_s = 1$ can be adopted as amplification factor of the bridge rectifier here [2].

3.2. Auto-controlled synchronous motor transfer function

When the system works normally, inverter bridge upper and lower arms each has one thyristor conducting, except at thyristor commutation stage, and the current passes through the two-phase stator armature winding of the synchronous motor. When the motor runs, the armature winding will produce induced EMF $e_{a\,b,c}$ and its effective value is supposed to be E. In analysis of the DC circuit, relationship between voltages at input and output side of the inverter bridge under steady state shall meet:

$$E_D = \frac{3\sqrt{6}}{\pi} E \cos(\gamma - \frac{\mu}{2}) \cos(\frac{\mu}{2}) \,. \tag{3}$$

Where γ is the inverter lead angle and μ is commutation overlap angle of inverter bridge thyristor and can be calculated with the following formula:

$$\mu = \gamma_0 - \cos^{-1}(\cos(\gamma_0) + \frac{\omega_1 L_c}{\sqrt{6}E_0} I_D) \,. \tag{4}$$

Relationship between currents at input and output side of inverter under steady state shall meet:

$$I_D = \frac{\pi}{\sqrt{6}} I \,, \tag{5}$$

Where I is effective value of current flowing into the motor stator.

With losses of inverter bridge and smoothing reactor ignored, motor input power can be expressed as:

$$P = E_D I_D = 3EI \cos(\gamma - \frac{\mu}{2}) \cos(\frac{\mu}{2}) \,. \tag{6}$$

Figure 3 shows auto-controlled synchronous motor phasor diagram with stator winding internal resistance ignored. There is a phase difference δ, known as power angle, between armature back EMF E (equal to motor terminal voltage) with the motor loaded and E_0 with the motor under no load. With external power factor angle $\varphi = \gamma_c + \frac{\mu}{2} = \gamma - \frac{\mu}{2}$ and internal power factor angle $\phi = \gamma_c + \delta + \frac{\mu}{2} = \gamma_0 - \frac{\mu}{2}$ with motor current ahead of voltage, it can be seen that for the synchronous to realize inverter bridge commutation during auto-controlled variable frequency startup, the current should be ahead of the voltage for certain phase and the motor should be capacitive.

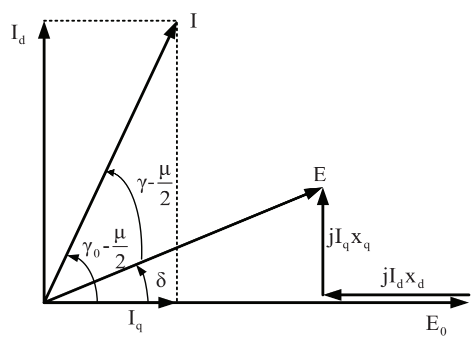

Fig. 3. Synchronous Motor Phasor Diagram

Based on the above figure, the formula for computing electromagnetic torque can be obtained, as follows:

$$T_e = \frac{3I}{n_p}\left(C_e - (L_d - L_q)\frac{\sqrt{6}}{\pi}I_D \sin(\gamma_0 - \frac{\mu}{2})\right)\cos(\gamma_0 - \frac{\mu}{2})\cos\frac{\mu}{2}\,, \tag{7}$$

Where C_e is EMF coefficient. It can be seen that when commutation overlap angle is taken into account, the computation of electromagnetic torque of the load commutated synchronous motor is quite complicated and it mainly consists of the following two parts: the electromagnetic torque produced by interaction between excitation field and stator field and reluctance torque produced by motor rotor saliency effect. For cylindrical synchronous motors, quadrature- and direct-axis reactance is equal and hence the reluctance torque is zero. Reluctance torque is generally small and, to simplify the model, can be ignored. Then, synchronous motor electromagnetic torque formula is similar to that of DC motor torque formula, as follows:

$$T_e = \frac{3}{n_p}C_e I\cos(\gamma_0 - \frac{\mu}{2})\cos\frac{\mu}{2}\,. \tag{8}$$

The relationship between motor phase EMF E and no-load EMF E_0 can be obtained from the phasor diagram and the following formula can be obtained by combining approximate treated electromagnetic torque formula:

$$E_D = \frac{3\sqrt{6}}{\pi}E\cos(\gamma_0 - \frac{\mu}{2})\cos\frac{\mu}{2}\,. \tag{9}$$

Under normal conditions, current of the double closed loop system has good dynamic performance and disturbance resistance. For design of regulator, commutation angles μ and μ_s and impact of reluctance torque can be ignored and $\gamma_0 = 60°$ adopted. The following can be obtained based on Laplace transform of formula (3-9) and variable substitution:

$$\frac{E_0(s)}{\frac{\sqrt{6}}{\pi}I_D(s) - I_L(s)} = \frac{R_\Sigma}{T_m s}\,, \tag{10}$$

Where: electromechanical time constant: $T_m = \frac{GD^2 R_\Sigma}{375 C_e C_m}$; Electromagnetic time constant $T_l = \frac{L}{R_\Sigma}$, and Torque coefficient $C_m = \frac{90}{\pi}\left(\cos\gamma_0 - \frac{\mu}{2}\right)C_e$.

To sum up, load commutated synchronous motor can be described with dynamic structure diagram according to the transfer function obtained, as shown in Figure4.

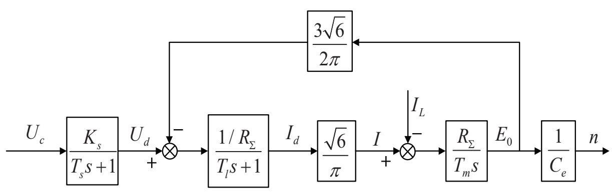

Fig. 4. Load Commutated Synchronous Motor Dynamic Structure Diagram

4. Basic operating characteristics of static variable frequency speed regulation system

4.1. Speed regulating characteristics

$$n = \frac{2.34U_s\cos(\alpha - \frac{\mu_s}{2})\cos(\frac{\mu_s}{2}) - I_D R_\Sigma}{2.34C_e\cos(\gamma_0 - \frac{\mu}{2})\cos(\frac{\mu}{2})}\,, \tag{11}$$

Where C_e is the coefficient of potential and it can be a constant under constant magnetic flux conditions. It can be seen from the formula that when the impact of commutation angles μ and μ_s is ignored, speed regulating characteristics of synchronous motor static variable frequency speed regulation system are similar to that of the DC motor.

4.2. Torque characteristics

As mentioned above, with impact of reluctance torque ignored, electromagnetic torque formula is as follows:

$$T_e = \frac{3}{n_p}C_e I_D\cos(\gamma_0 - \frac{\mu}{2})\cos(\frac{\mu}{2})\,. \tag{12}$$

It can thus be seen that, with no-load commutation lead angle γ_0 unchanged, synchronous motor electromagnetic torque is proportional to DC bus current I_D and torque ripple corresponds to motor stator current ripple and harmonic content.

In conclusion, load commutated static variable frequency speed regulation system has speed regulating characteristics similar to that of DC motors and is featured with simple AC motor structure, easy manufacture and maintenance, high synchronous motor power factor and other advantages. Hence, load commuted synchronous motors have been widely used in adjustable speed drive region requiring large capacity, high speed and high performance and played a special role in large synchronous motor soft start.

5. Double closed loop control of SFC start

According to basic operating characteristic analysis of the above section, if rotor flux and no-load commutation lead angle γ_0 remain unchanged, electromagnetic torque required for accelerated start can be controlled by controlling DC bus current I_D. Similar to DC motor closed loop speed regulation system, speed and current double closed loop control is required to be introduced to realize control of current during start and static error free speed when synchronous speed is achieved [3].

Figure 5 shows the actual dynamic structure diagram of the load commutated synchronous motor double closed loop speed regulation system with filter delay in current and speed detection links taken into account. It can be seen from the figure that the simplified synchronous motor speed regulation system has control structure

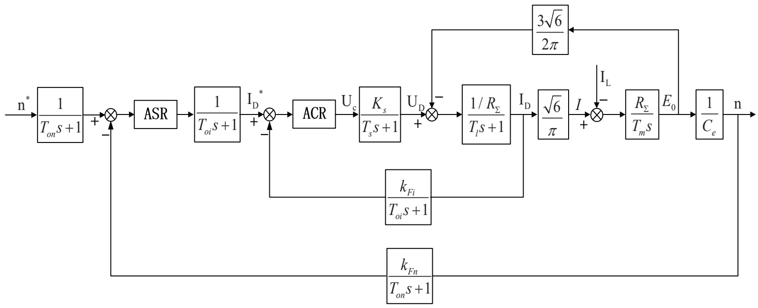

Fig. 5. Structure Diagram of Load Commutated Synchronous Motor Double Closed Loop Speed Regulation System

model similar to that of DC motor closed loop speed regulation system. Therefore, mature engineering design methods of the DC motor double closed loop speed regulation system can be employed for regulator design.

6. Practical applications of double closed loop controllers

Figure 6 shows schematic diagram of SFC in actual use and the AC-DC-AC mode is adopted. It consists of step-down transformer, rectifier thyristor DC smoothing reactors, thyristor inverters, boosting transformer, synchronous cutting-in device, rotor position detection and other components and forms Y and ΔIoops. Variable frequency starting comprises five processes: rotor starting, low-speed starting, high-speed starting, synchronous adjustment and cutting-in. Output current is adjusted through real-time tracking of motor rotor position, thus preventing out of step [4]. Both Y and ΔIoops adopt double closed loop control and adjust output frequency according to starting speed curve given prior to starting to get the motor run at full speed within given time.

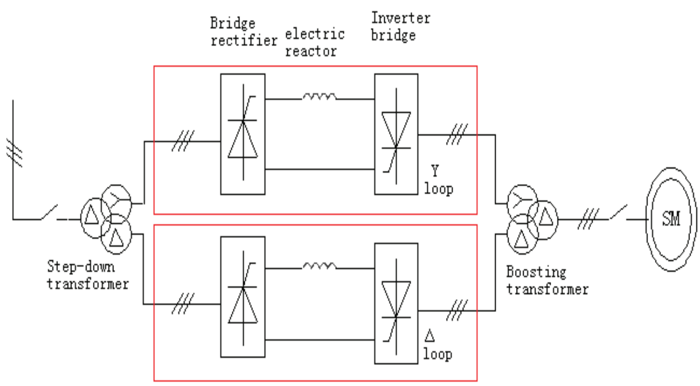

Fig. 6. SFC Schematic Diagram

This test platform adopts a 40000kW synchronous motor with rated speed being

3000rpm, rated voltage being 10kV and rated exciting current being 150A. As for the test results, Figure 7 indicates the waveform recorded by the oscilloscope during starting of the motor. Green line: Δloop grid side line AB voltage; yellow line: Δloop inverter side line UV voltage; red: Y loop DC side current; blue: Δloop DC side current.

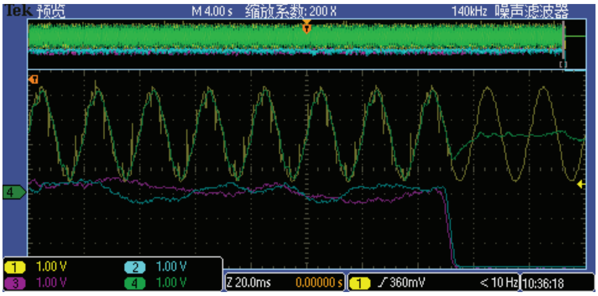

Fig. 7. Waveform Recorded by Oscilloscope during Starting of Motor

Figure 8 indicates starting speed and DC side current curves. The green line shows motor speed; blue line is Δloop DC side current curve and red line is Y loop DC side current. It can be seen that both loops are basically consistent in the starting process and motor speed ramps up. Cutting-in is achieved when it approximates rated speed and the motor starts operating at industrial frequency.

Fig. 8. Starting Speed and Y and ΔLoop DC Side

7. Conclusion

SFCs have unparalleled advantages among all modes of starting of large synchronous motors. Yet, domestic SFC market is mainly occupied by several foreign manufacturers. Through analysis of synchronous motor SFC control policies, this paper introduces the design of a double closed loop controller. Based on analysis of electromagnetic torque during starting of the synchronous motor and introduction of speed and current double closed loop control, this design is proven to be able to realize current control during starting and static error free speed when synchronous speed is achieved. In practice, this method has been successfully used for variable frequency starting at the second blast station of a thermal plant of Wuhan Iron and Steel (Group) Corp. and has provided reliable theoretical basis for SFC control policies.

References

[1] P. Li, C. J. Li, C. Y. Zhu. *Commutation Analysis of Load Commutated Synchronous Motor Speed Regulation System*[C]. 2010 Annual Meeting of Nationwide Metallurgical Industry Automation Information Network, Qingdao, (2010), 526–529.

[2] Z. H. Lu. *Application and Research of the High-voltage Converter Soft-starter in Synchronization Motor.* Master's Thesis of Shandong University, Qingdao, (2009), 17–59.

[3] H. J. Du. *Research on High Voltage Commutatorless Motor and Its Control.* Doctoral Dissertation of North China Electric Power University, Baoding, (2005), 23–49, 64–77.

[4] X. K. He. *Static Frequency Conversion Starting of Pumped-storage Machine.* Master's Thesis of Huazhong University of Science and Technology, Wuhan, (2006), 10–41.

Received September 12, 2017